

International Journal of Innovative Research in Science, Engineering and Technology

(A High Impact Factor, Monthly, Peer Reviewed Journal)

Visit: www.ijirset.com

Vol. 8, Issue 5, May 2019

Segmentation of Outer Retinal Layers Using Model Selection Algorithms

T. Shanmugavalli¹, K.Sridar²

PG Scholar, Veerammal Engineering College, K. Singarakottai, Tamil Nadu, India¹

Assistant Professor, Department of CSE, Veerammal Engineering College, K. Singarakottai, Tamil Nadu, India²

ABSTRACT: Extraction of image-based biomarkers, such as the presence, visibility or thickness of a certain layer, from 3D optical coherence tomography data provides relevant clinical information. We present a method to simultaneously determine the number of visible layers in the outer retina and segment them. The method is based on a model selection approach with special attention given to the balance between the quality of a fit and model complexity. This will ensure that a more complex model is selected only if this is sufficiently supported by the data. The performance of the method was evaluated on healthy and retinitis pigmentosa (RP) affected eyes. Additionally, the reproducibility of automatic method and manual annotations was evaluated on healthy eyes. A good agreement between the segmentation performed manually by a medical doctor and results obtained from the automatic segmentation was found. The mean unsigned deviation for all outer retinal layers in healthy and RP affected eyes varied between 2.6 and 4.9 μm . The reproducibility of the automatic method was similar to the reproducibility of the manual segmentation. Overall, the method provides a flexible and accurate solution for determining the visibility and location of outer retinal layers and could be used as an aid for the disease diagnosis and monitoring.

KEYWORDS: Akaike information criteria, Attenuation coefficient, Bayesian information criteria, Information complexity, Maximum likelihood estimation, Model selection, Retinitis pigmentosa.

I. INTERODUCTION

OPTICAL coherence tomography (OCT) is a non-invasive, non-contact, optical imaging technique that can be used to acquire in-vivo images of retinal structures [1]. Due to its high axial resolution and sensitivity, different cell layers that compose the retina, can be visualized by differences in backscattering, as is shown in Figure 1a. Hence, the effect of retinal diseases on both the inner, anterior and the outer, posterior retinal layers can be investigated. Retinitis pigmentosa (RP), age-related macular degeneration (AMD) and Stargardt disease (SD) are among those eye dis-eases that cause anatomical changes in the outer retinal layers. Retinal OCT images of RP subjects show that the external limiting membrane (ELM) and the ellipsoid zone (EZ) become dimmer or even completely disappear [2]–[4], whereas OCT scans of SD show that ELM and the retinal pigment epithelium (RPE) change in thickness [5], [6]. Therefore, presence, visibility and thickness of these outer retinal layers are potential biomarkers that can aid in the diagnosis and monitoring of retinal diseases. Manual annotations and extraction of these image-based biomarkers can be tedious, time consuming and subjective. To provide an objective assessment of the relevant retinal layers and thereby an objective quantification of the biomarkers, automatic segmentation methods are required. Automatic segmentation of the layers in the outer retina can be challenging for the following two reasons. First, the layers are often indiscernible due to the limited resolution of the eye's optics and the OCT system [7]. Second, layers may deteriorate as a result of a disease [2], [6], [8]. Indeed, Lang et al. reported that segmentation of missing layers might be problematic [9]. Although many automatic algorithms for the segmentation of retinal layers have been developed [10]– [20], only three addressed the problem of vanishing layers [21]–[23]. First, Yang et al. [21] segmented the layers of the outer retina in a sequential manner by using a dual gradient and shortest path search in which some of the layers were allowed to overlap. However, in their approach the ELM, was not segmented, although it is of interest in both RP and SD.

International Journal of Innovative Research in Science, Engineering and Technology

(A High Impact Factor, Monthly, Peer Reviewed Journal)

Visit: www.ijirset.com

Vol. 8, Issue 5, May 2019

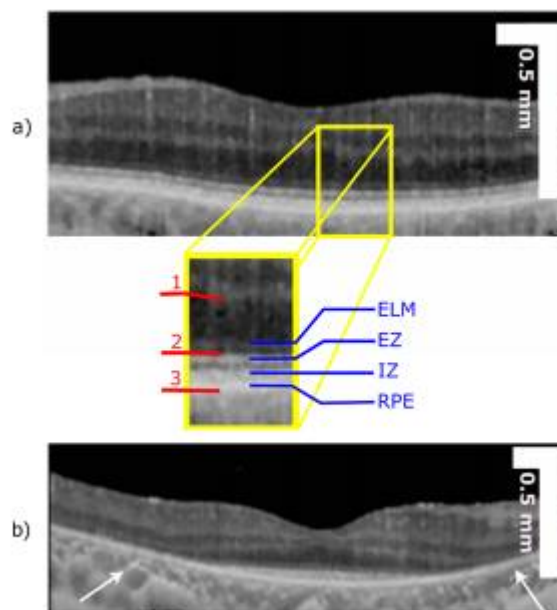


Fig. 1: An OCT B-scan of a healthy (a) and RP (b) affected retina after conversion to attenuation coefficient (see section III-A). The arrows point to areas where several outer retinal layers are no longer visible. Boundaries marked with red lines are obtained with our previously proposed method (see section III-A) and are used to define the region of interest (the outer retina). The abbreviations of these interfaces are as follows: 1. OPL - ONL interface, 2. anterior EZ boundary and 3. Posterior RPE boundary. The outer retinal layers and their abbreviations are indicated with blue lines.

Clustering Based Segmentation

Clustering is nothing but an attempt in which measurement points or patterns are grouped together. This technique is generally applied for data of n dimension. This n corresponds to an arbitrary number, i.e. it can be two, three or more. The clustering technique is best suited for sparse type of images. This technique includes methods like kmeans, fuzzy c-means etc. Subrajeet Mohapatra & Deepti Patra proposed an automated nucleus segmentation method. In the proposed technique, two step segmentation is done to segment a WBC nucleus from rest of the image objects. In first stage an initial segmentation is performed by executing a semi supervised k-means clustering. The next stage is a follow up of first step in which a second stage of segmentation is done using nearest neighbor classification in L^*a*b space.

In a clustering based approach is used to segment white blood cells in blood microscopic images. In the proposed system, first the image is converted into Lab color space. Then a fuzzy kmeans clustering is carried out that divide the image into 3 clusters. Simultaneously an automatic histogram based thresholding is also performed on the Lab color image. The two results i.e. clusters and the reference image (obtained after applying threshold) are compared, selected and a logical AND operation is performed. The resulting image is a clean segmented image. The approach presented is used to detect AML (Acute Myelogenous Leukemia) in microscopic images of blood. Three clusters are identified which represent nucleus, background and other cells like erythrocytes, leukocytes etc. Every pixel of the image is assigned to one of these clusters based on the cluster property. The technique performs some preprocessing followed by k-means clustering for segmentation purpose. The segmentation is performed to extract the leukocytes' nuclei using color based clustering. S. Schupp et al. presented a system of automatic microscopic image segmentation combining fuzzy clustering and active contour model. An automatic initialization algorithm based on fuzzy clustering is used to robustly identify and classify all possible seed region in the image. This seed are propagated outward simultaneously to localize the final contour of all objects.

International Journal of Innovative Research in Science, Engineering and Technology

(A High Impact Factor, Monthly, Peer Reviewed Journal)

Visit: www.ijirset.com

Vol. 8, Issue 5, May 2019

II. LITERATURE SURVAY

PAPER-1 SEGMENTATION OF 4D CARDIAC MRI: AUTOMATED METHOD BASED ON SPATIO-TEMPORAL WATERSHED CUTS

We propose a new automated and fast procedure to segment the left ventricular myocardium in 4D MRI sequences. Both quantitative and qualitative evaluations are provided. We demonstrate the accuracy of the proposed method. Here we used discrete mathematical morphology. The time efficiency is high. The accuracy of the automated method compared to manual segmentations performed by two cardiologists; the ability of the method to compute reliable characteristics of the LV (ejection fraction and left ventricular mass); the temporal continuity of the resulting automated segmentation; the time-efficiency (about 3' to segment a sequence of 25 3D-images on a low-end computer) of the proposed method; and the robustness of the few parameters whose setting rely mostly on physical and anatomical facts. MR images of the LV, together with three associated segmentations: two handmade segmentations – each one of them performed by an independent and blinded expert cardiologist and one 4D automated segmentation obtained by the proposed method. The first objective of this paper is to show that mathematical morphology offers interesting alternatives to these approaches in the important and difficult task of designing cardiac segmentation methods that can be used in clinical routine. We introduced the watershed cuts, a notion of watershed in edge-weighted graphs which is optimal in a sense equivalent to minimum spanning trees. This paper presents the first application of this new paradigm. Furthermore, this paper introduces the watershed-cuts in 4-dimensional spaces (3D+time). Our second objective is to show the ability of this operator to take into account both the spatial and temporal gradient of the images and therefore its ability to produce segmentations that are spatially as well as temporally consistent. The proposed method is evaluated on cine-MR image following by this sequence

- the accuracy of the automated method compared to manual segmentations performed by two cardiologists;
- the ability of the method to compute reliable characteristics of the LV (ejection fraction and left ventricular mass);
- the temporal continuity of the resulting automated segmentation;
- the time-efficiency (about 3' to segment a sequence of 25 3D-images on a low-end computer) of the proposed method; and
- The robustness of the few parameters whose setting rely mostly on physical and anatomical facts.

Since it is independent of any high-level model, the proposed method can be used to fairly assess model-based segmentation schemes by comparing their results with our non-model based segmentation, hence, discarding bias due to the choice of different models. Furthermore, the proposed method can be used to register generic physiological models of the heart to real patient specific cardiac images. In general, it is indeed easier to register a model to a binary segmentation than directly to images. So we introduce in this paper a new watershed framework which allows for segmenting spatio-temporal images that we apply to medical image analysis. Specifically, we propose a new automated and fast procedure to segment the left ventricular myocardium in 4D (3D+t) cine-MRI sequences. The successive segmentations obtained over the time take into account spatio-temporal properties of the images. Thanks to the comparison with manual segmentation performed by two cardiologists, we demonstrate the accuracy of the proposed method and the relevance of the ejection fraction and myocardium mass derived from the automated segmentations. Therefore, this automated method can be used in clinical routine. The proposed scheme does not permit the direct derivation of deformation parameters. Such deformation parameters can be obtained thanks to a model of the heart movement, and such a heart model needs the obtained segmentations as control points. Future work will aim at computing deformation fields whose accuracy will be improved by registration with other modalities such as delayed enhanced MRI and CT scan.

DISADVANTAGE

- In the scheme does not permit the direct derivation of deformation parameters.
- Registration accuracy is low

International Journal of Innovative Research in Science, Engineering and Technology

(A High Impact Factor, Monthly, Peer Reviewed Journal)

Visit: www.ijirset.com

Vol. 8, Issue 5, May 2019

- To improve by registration with other modalities such as delayed enhanced MRI and CT scan

PAPER -2 A REVIEW OF SEGMENTATION METHODS IN SHORT AXIS CARDIAC MR IMAGES

This paper is a review of fully and semi-automated methods performing segmentation in short axis images using a cardiac cine MRI sequence. We will review automatic and semi-automatic segmentation methods of cine MR images of the cardiac ventricles, using the short-axis view. The wide variety of image-driven approaches using weak or no prior have been proposed to tackle the ventricle segmentation in cardiac MRI. Almost all of these methods require either minimal or great user intervention. If image based and pixel classification-based approaches offer a limited framework for incorporating strong prior, straightforward extensions of deformable models in this sense have been extensively studied. In the next section are presented Methods relying on strong prior for heart segmentation. It can be generated by manually segmenting an image or by integrating information from multiple segmented images from different individuals. Strong prior based methods can overcome the previously defined segmentation problems.

- (i) No information is used, but our study shows that in this case user interaction is required
- (ii) Weak prior, that is, low level information such as geometrical assumptions on the ventricle shape, often combined to low-level user interaction,
- (iii) Strong prior such as statistical models, constructed or learned from a large number of manually segmented images, not requiring user interaction.

Our image segmentation categorization includes on the one hand image-driven and pixel classification based approaches, and deformable models, making use of weak or no prior.

DISADVANTAGE

- This particularly complex segmentation task, prior knowledge is required.
- Major challenges linked to this segmentation task.
- Image processing and pattern recognition problems are occurring.

PAPER-3 MULTI-ATLAS SEGMENTATION OF THE PROSTATE: A ZOOMING PROCESS WITH ROBUST REGISTRATION AND ATLAS SELECTION

This paper presents a multi-atlas-based automatic pipeline for segmenting prostate in MR images. Image registration is needed to transfer expert defined ground-truth prostate segmentation from atlases onto target image. However, registration is rendered difficult in this dataset, due to different images having different field of view (FOV), different imaging protocol (from multiple imaging centers), and large anatomical variability around prostate and large pathologic variability (some having enlarged prostate or prostate cancer). To overcome these limitations, we propose a "zooming process" for multi-atlas-based prostate segmentation. We first register all atlases onto target image to obtain an initial segmentation of the prostate. This step includes robust registration, atlas selection and majority-based label fusion. Then, we "zoom-in": re-run all atlas-to-target registrations, but this time restricting the registration to the vicinity of the prostate, ignoring compounding structures that are far away from the prostate and are largely variable. As a result, we can expect more accurate registrations and hence refined prostate segmentation. Our cross-validated results show improvement in segmentation by robust registration and atlas selection, compared to using all atlases. Additional improvement is observed when zooming in and focusing on registration of the prostate vicinity. We report average 0.84 dice overlap with expert-defined prostate segmentation in training subjects. Accuracy in testing datasets will be released by organizers of this challenge. This paper proposed a fully automatic pipeline for segmenting prostate MR images. We made two contributions in this study. The first is using robust image registration and especially atlas selection in multi-atlas-based segmentation framework. Due to large variability in prostate images across subjects, failure in atlas-to-target registration is not uncommon. Therefore, using robust image registration method to reduce the number of failures and developing criterion for removing failed atlases become key to accurate segmentation. Our second contribution is the development of a zooming process and its proof of concept. The idea is to focus on registration of the prostate vicinity, in the hope of improving registration accuracy in prostate regions and hence the accuracy in segmentation. By doing so, we largely reduce the negative impact from those highly variable structures far away from the prostate. As a result, we observed significant improvement in segmentation accuracy.

International Journal of Innovative Research in Science, Engineering and Technology

(A High Impact Factor, Monthly, Peer Reviewed Journal)

Visit: www.ijirset.com

Vol. 8, Issue 5, May 2019

III. METHODOLOGY & IMPLEMENTATION

1. PREPROCESSING

The Blood cell image is taken as input. Because these data are collected from outside sources, Since diffraction effects are almost always negligible once the blood cell is of visible size, we use the disc function to approximate the real image in our experiments. Even though the actual MRI image for cameras used for the test images are unknown, the disc approximation seems to be quite adequate. Our method still get the amount of local blood cell images for all these test images, depicts 3D geometric information for each scene, and does a good job in identifying in-focus subjects.

2. FEATURES EXTRACTION

Feature extraction in image processing is a technique of redefining a large set of redundant data into a set of features of reduced dimension. Transforming the input data into the set of features is called feature extraction. Feature selection greatly influences the classifier performance; therefore, a correct choice of features is a very crucial step. In order to construct an effective feature set, several published articles were studied, and their feature selection methodology was observed. It was noted that certain features were widely used as they gave a good classification. We implemented these features on whole images in our system. Those features were considered to boost the classifier performance.

Use analysis techniques on a segmented image to mark the location and size of complete and non overlapping cells in a microscopic image.

Green plane feature extraction, Shade correction, Executed detection output will shows like below images

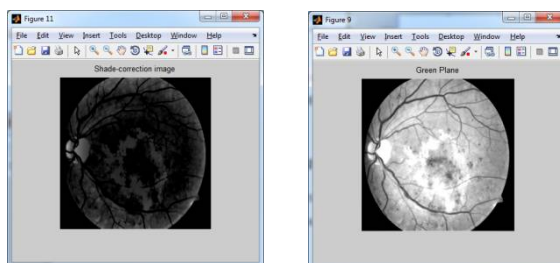


FIG2 GREEN PLANE EXTRACTION

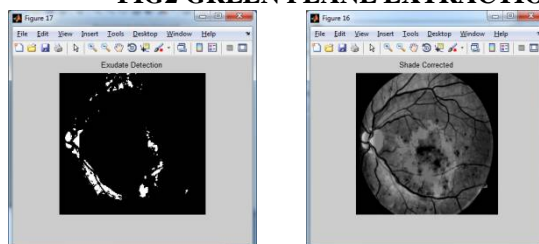


Fig3 Execution Detection

3. CELL FEATURES SEGMENTED

A least-squares partitioning method that divide a collection of objects into the groups. The algorithm iterates over two steps:

1. Compute the mean of each cluster.
2. Compute the distance of each point from each cluster by computing its distance from the corresponding cluster mean. Assign each point to the cluster it is nearest to.
3. Iterate over the above two steps till the sum of squared within group errors cannot be lowered any more.

International Journal of Innovative Research in Science, Engineering and Technology

(A High Impact Factor, Monthly, Peer Reviewed Journal)

Visit: www.ijirset.com

Vol. 8, Issue 5, May 2019

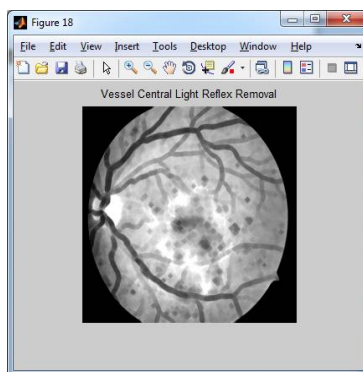


Fig4 Vessels removal

The initial assignment of points to clusters can be done randomly. In the course of the iterations, the algorithm tries to minimize the sum, over all groups, of the squared within group errors, which are the distances of the points to the respective group means. Convergence is reached when the objective function (i.e., the residual sum-of-squares) cannot be lowered any more. The groups obtained are such that they are geometrically as compact as possible around their respective means.

4. CLASSIFIED FEATURES

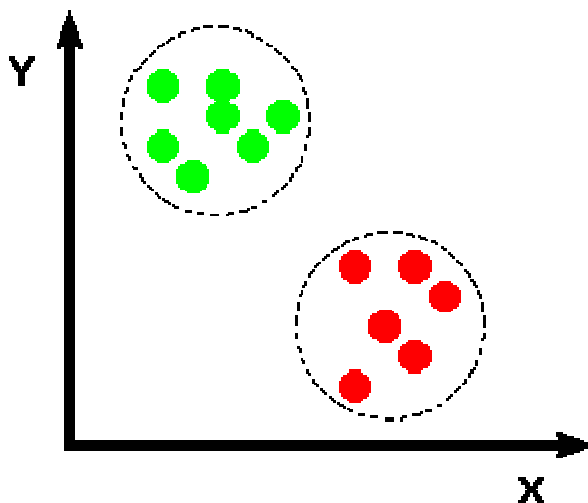


Fig5 classification

Common Names: Classification

Classification includes a broad range of decision-theoretic approaches to the identification of images (or parts thereof). All classification algorithms are based on the assumption that the image in question depicts one or more features (*e.g.*, geometric parts in the case of a manufacturing classification system, or spectral regions in the case of remote sensing, as shown in the examples below) and that each of these features belongs to one of several distinct and exclusive classes.

International Journal of Innovative Research in Science, Engineering and Technology

(A High Impact Factor, Monthly, Peer Reviewed Journal)

Visit: www.ijirset.com

Vol. 8, Issue 5, May 2019

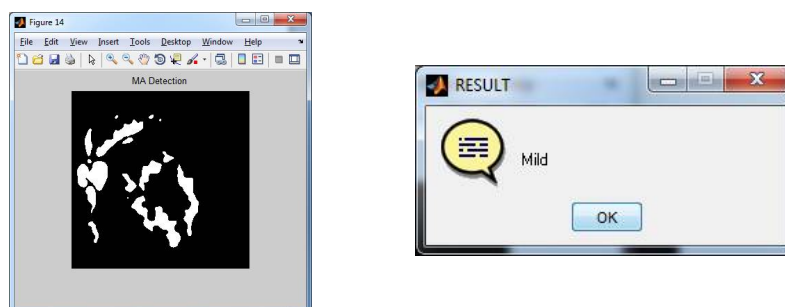


Fig 6 MA Detection

The classes may be specified *a priori* by an analyst (as in *supervised classification*) or automatically clustered (*i.e.* as in *unsupervised classification*) into sets of prototype classes, where the analyst merely specifies the number of desired categories. (Classification and *segmentation* have closely related objectives, as the former is another form of component labeling that can result in segmentation of various features in a scene.)

Process:

Image classification analyzes the numerical properties of various image features and organizes data into categories. Classification algorithms typically employ two phases of processing: *training* and *testing*. In the initial training phase, characteristic properties of typical image features are isolated and, based on these, a unique description of each classification category, *i.e.* *training class*, is created. In the subsequent testing phase, these feature-space partitions are used to classify image features.

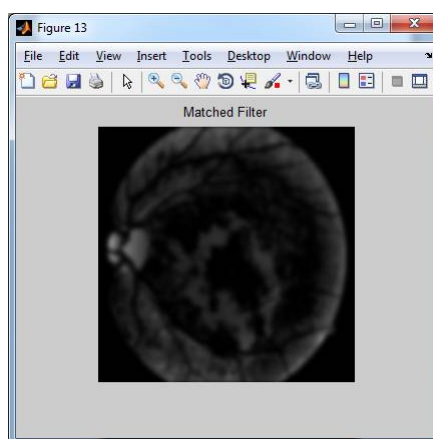


Fig 7 Matched Filter

The description of training classes is an extremely important component of the classification process. In supervised classification, *statistical* processes (*i.e.* based on an *a priori* knowledge of probability distribution functions) or *distribution-free* processes can be used to extract class descriptors. Unsupervised classification relies on *clustering* algorithms to automatically segment the training data into prototype classes. In either case, the motivating criteria for constructing training classes is that they are:

- *independent*, *i.e.* a change in the description of one training class should not change the value of another,
- *discriminatory*, *i.e.* different image features should have significantly different descriptions, and

International Journal of Innovative Research in Science, Engineering and Technology

(A High Impact Factor, Monthly, Peer Reviewed Journal)

Visit: www.ijirset.com

Vol. 8, Issue 5, May 2019

- *reliable*, all image features within a training group should share the common definitive descriptions of that group.

A convenient way of building a parametric description of this sort is via a feature vector (v_1, v_2, \dots, v_n) , where n is the number of attributes which describe each image feature and training class. This representation allows us to consider each image feature as occupying a point, and each training class as occupying a sub-space (*i.e.* a representative point surrounded by some spread, or deviation), within the n -dimensional classification space. Viewed as such, the classification problem is that of determining to which sub-space class each feature vector belongs.

5. CLASSIFICATION

This classification result gives the details about retinitis pigmentosa affected eyes and nonretinitis pigmentosa affected eyes blood cells. To get the spitted part from the k means segmentation result. Above the result which is used to find the retinitis pigmentosa affected eyes and nonretinitis pigmentosa affected eye cells from this module. Classification result generates the kmeans cluster and also use SVM (Support vector machine).

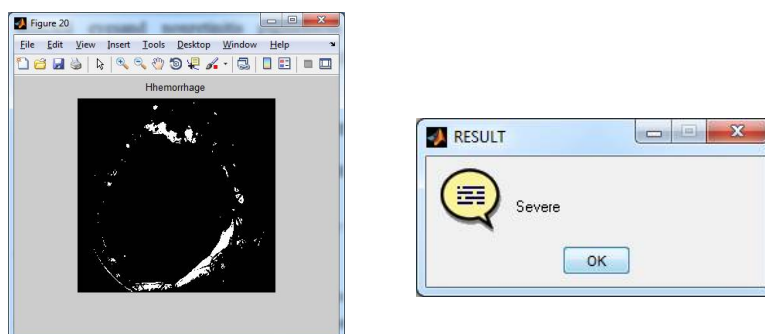


Fig 7 Classification Result

IV. CONCLUSION AND FUTURE ENHANCEMENT

CONCLUSION

In this paper we have proposed a framework for comparing image segmentation algorithms, and performed one such comparison. Our framework consists of comparing the performance of segmentation algorithms based on three important characteristics: correctness, stability with respect to parameter choice, and stability with respect to image choice. If an algorithm performs well with respect to all of these characteristics, it has the potential to be useful as part of a larger vision system.

Image segmentation has become a very important task in today's scenario. In the present day world computer vision has become an interdisciplinary field and its applications can be found in any area be it medical, remote sensing, electronics and so on. Thus, to find an appropriate segmentation algorithm based on your application and the type of inputted image is very important.

The presented system performs automated processing, including color correlation, segmentation of the nucleated cells, and effective validation and classification. A feature set exploiting the shape, color, and texture parameters of a cell are constructed to obtain all the information required to perform efficient classification. The impact of the Clustering operator on the FD proved to be a promising feature for this analysis. Furthermore, a color feature called cell energy was introduced, and results show that this feature presents a good demarcation between retinitis pigmentosa affected eyes and non affected eyes.

International Journal of Innovative Research in Science, Engineering and Technology

(A High Impact Factor, Monthly, Peer Reviewed Journal)

Visit: www.ijirset.com

Vol. 8, Issue 5, May 2019

FUTURE ENHANCEMENT

In this project we detect the affected part on a MR image. And to find the connection between the probabilistic label fusion model and the recently proposed kmeans segmentation method. Another contribution is that label information is incorporated into image registration to improve registration accuracy. Experimental results show that registration refinement improves segmentation accuracy. The method produces reliable clinical indexes which are in good agreement with the manual measurements. It can provide useful information for clinicians in retinitis pigmentosa affected eyes disease diagnosis.

REFERENCES

- [1] J. Cousty, L. Najman, M. Couprie, S. Clément-Guinaudeau, T. Goissen, and J. Garot, "Segmentation of 4D cardiac MRI: Automated method based on spatio-temporal watershed cuts,"
- [2] M. Jolly, "Fully automatic left ventricle segmentation in cardiac cine MR images using registration and minimum surfaces," MIDAS.
- [3] M. Lorenzo-Valdés, G. I. Sanchez-Ortiz, A. G. Elkington, R. H. Mohiaddin, and D. Rueckert, "Segmentation of 4D cardiac MR images using a probabilistic atlas and the EM algorithm,"
- [4] M. Lynch, O. Ghita, and P. F. Whelan, "Segmentation of the left ventricle of the heart in 3- MRI data using an optimized Nonrigid Temporal model,"
- [5] C. Petitjean and J. N. Dacher, "A review of segmentation methods in short axis cardiac MR images,"
- [6] T. R. Burke, D. W. Rhee, R. T. Smith, S. H. Tsang, R. Allikmets, S. Chang, M. A. Lazow, D. C. Hood, and V. C. Greenstein, "Quantification of peripapillary sparing and macular involvement in stargardt disease (STGD1)," *Investigative Ophthalmology and Visual Science*, vol. 52, no. 11, pp. 8006–8015, 2011.
- [7] R. F. Spaide and C. A. Curcio, "Anatomical correlates to the bands seen in the outer retina by optical coherence tomography: Literature review and model," *Retina*, vol. 31, no. 8, pp. 1609–1619, 2011.
- [8] E. Ergun, B. Hermann, M. Wirtitsch, A. Unterhuber, T. H. Ko, H. Sattmann, C. Scholda, J. G. Fujimoto, M. Stur, and W. Drexler, "Assessment of central visual function in stargardt's disease/fundus flavimaculatus with ultrahigh-resolution optical coherence tomography," *Investigative Ophthalmology and Visual Science*, vol. 46, no. 1, pp. 310–316, 2005.
- [9] A. Lang, A. Carass, M. Hauser, E. S. Sotirchos, P. A. Calabresi, H. S. Ying, and J. L. Prince, "Retinal layer segmentation of macular OCT images using boundary classification," *Biomedical Optics Express*, vol. 4, no. 7, pp. 1133–1152, 2013.
- [10] R. Kafieh, H. Rabbani, and S. Kermani, "A review of algorithms for segmentation of optical coherence tomography from retina," *Journal of Medical Signals and Sensors*, vol. 3, no. 1, pp. 45–60, 2013.
- [11] D. C. DeBuc, "A review of algorithms for segmentation of retinal image data using optical coherence tomography." In *Tech*, 2011, vol. 6688, ch. 2, pp. 14–54.
- [12] K. A. Vermeer, J. van der Schoot, H. G. Lemij, and J. F. de Boer, "Automated segmentation by pixel classification of retinal layers in ophthalmic OCT images," *Biomedical Optics Express*, vol. 2, no. 6, pp. 1743–1756, 2011.
- [13] M. Mujat, R. C. Chan, B. Cense, B. Hyle Park, C. Joo, T. Akkin, T. C. Chen, and J. F. de Boer, "Retinal nerve fiber layer thickness map determined from optical coherence tomography images," *Optics Express*, vol. 13, no. 23, pp. 9480–9491, 2005.
- [14] M. A. Mayer, J. Hornegger, C. Y. Mardin, and R. P. Tornow, "Retinal nerve fiber layer segmentation on FD-OCT scans of normal subjects and glaucoma patients," *Biomedical Optics Express*, vol. 1, no. 5, pp. 1358–1383, 2010.
- [15] J. Novosel, G. Thepass, H. G. Lemij, J. F. de Boer, K. A. Vermeer, and L. J. van Vliet, "Loosely coupled level sets for simultaneous 3D retinal layer segmentation in optical coherence tomography," *Medical Image Analysis*, vol. 26, no. 1, pp. 146–158.
- [16] H. Ishikawa, D. M. Stein, G. Wollstein, S. Beaton, J. G. Fujimoto, and J. S. Schuman, "Macular segmentation with optical coherence tomography," *Investigative Ophthalmology and Visual Science*, vol. 46, no. 6, pp. 2012–2017, 2005.
- [17] P. A. Dufour, L. Ceklic, H. Abdillahi, S. Schroder, S. De Dzanet, U. Wolf-Schnurrbusch, and J. Kowal, "Graph-based multi-surface segmentation of OCT data using trained hard and soft constraints," *Medical Imaging, IEEE Transactions on*, vol. 32, no. 3, pp. 531–543, 2013.
- [18] A. Carass, A. Lang, M. Hauser, P. A. Calabresi, H. S. Ying, and J. L. Prince, "Multiple-object geometric deformable model for segmentation of macular OCT," *Biomedical Optics Express*, vol. 5, no. 4, pp. 1062–1074, 2014.
- [19] S. J. Chiu, X. T. Li, P. Nicholas, C. A. Toth, J. A. Izatt, and S. Farsiu, "Automatic segmentation of seven retinal layers in SD-OCT images congruent with expert manual segmentation," *Optics Express*, vol. 18, no. 18, pp. 19 413–19428, 2010.
- [20] M. Garvin, M. Abramoff, R. Kardon, S. Russell, X. Wu, and M. Sonka, "Intraretinal layer segmentation of macular optical coherence tomography images using optimal 3-D graph search," *Medical Imaging, IEEE Transactions on*, vol. 27, no. 10, pp. 1495–1505, 2008.
- [21] Q. Yang, C. A. Reisman, K. Chan, R. Ramachandran, A. Raza, and D. C. Hood, "Automated segmentation of outer retinal layers in macular OCT images of patients with retinitis pigmentosa," *Biomedical Optics Express*, vol. 2, no. 9, pp. 2493–2503, 2011.
- [22] R. Kafieh, H. Rabbani, M. D. Abramoff, and M. Sonka, "Intra-retinal layer segmentation of 3D optical coherence tomography using coarse grained diffusion map," *Medical Image Analysis*, vol. 17, no. 8, 2013.
- [23] P. P. Srinivasan, S. J. Heflin, J. A. Izatt, V. Y. Arshavsky, and S. Farsiu, "Automatic segmentation of up to ten layer boundaries in SD-OCT images of the mouse retina with and without missing layers due to pathology," *Biomedical Optics Express*, vol. 5, no. 2, pp. 348–365, 2014.
- [24] K. A. Vermeer, J. Mo, J. J. A. Weda, H. G. Lemij, and J. F. de Boer, "Depth-resolved model-based reconstruction of attenuation coefficients in optical coherence tomography," *Biomedical Optics Express*, vol. 5, no. 1, pp. 322–337, 2014.
- [25] J. Novosel, K. Vermeer, L. Pierrache, C. Klaver, L. van den Born, and L. van Vliet, "Method for segmentation of the layers in the outer retina,"



ISSN(Online): 2319-8753
ISSN (Print): 2347-6710

International Journal of Innovative Research in Science, Engineering and Technology

(A High Impact Factor, Monthly, Peer Reviewed Journal)

Visit: www.ijirset.com

Vol. 8, Issue 5, May 2019

- in Engineering in Medicine and Biology Society (EMBC), 2015 37th Annual International Conference of the IEEE, Aug 2015, pp. 5646– 5649.
- [26] G. Staurengi, S. Sadda, U. Chakravarthy, and R. F. Spaide, “Proposed lexicon for anatomic landmarks in normal posterior segment spectral-domain optical coherence tomography,” *ophthalmology*, vol. 121, no. 8, pp. 1572–1578.
- [27] R. A. Fisher, “On the mathematical foundations of theoretical statistics,” *Philosophical Transactions of the Royal Society of London A: Mathematical, Physical and Engineering Sciences*, vol. 222, no. 594-604, pp. 309–368, 1922